

Translational and Rotational Diffusion of Probe Molecules in Polymer Films near T_g : Effect of Hydrogen Bonding

David B. Hall,[†] Kenneth E. Hamilton,[†] Robert D. Miller,[‡] and John M. Torkelson^{*,†,§}

Department of Chemical Engineering, Northwestern University, Evanston, Illinois 60208; IBM Almaden Research Center, 560 Harry Rd., San Jose, California 95120; and Department of Materials Science and Engineering, Northwestern University, Evanston, Illinois 60208

Received March 22, 1999; Revised Manuscript Received October 5, 1999

ABSTRACT: The effect of hydrogen bonding on the rotational and translational dynamics of two small molecule probes, lophine and *S*-lophine, in amorphous polymer films near the glass transition temperature, T_g , was studied using second harmonic generation (SHG) and fluorescence nonradiative energy transfer (NRET), respectively. The two probes are nearly identical in size and shape, with the only structural difference being related to an amine functional group in lophine replacing a sulfur atom in *S*-lophine. The two probes exhibited essentially identical rotational and translational dynamics in polystyrene, which has no polar units allowing for hydrogen-bonding interactions. However, in poly(isobutyl methacrylate), which can participate in hydrogen bonding with amine units, lophine average rotational reorientation times ($\langle\tau_{\text{rot}}\rangle$) were found to increase, and translational diffusion coefficients (D) were found to decrease by approximately an order of magnitude as compared to those of *S*-lophine. The magnitude of this effect is much greater than similar hydrogen-bonding effects reported for diffusion in polymer solutions. The hydrogen-bonding effects can be quantitatively taken into account using an interaction energy term with activation energy, $E_a = 6$ kJ/mol for translation and 9.5 kJ/mol for rotation. The differences in E_a for the two modes of motion are explained in terms of the differing ways in which D and $\langle\tau_{\text{rot}}\rangle$ average over the broad distribution of relaxation times present in polymers near T_g . Implications associated with additive migration in polymers are discussed.

Introduction

An understanding of small molecule or additive diffusion in polymer films is of importance to such diverse technologies as packaging,¹ drug delivery,² and nonlinear optics.^{3,4} Additionally, safety concerns have been raised regarding the migration of additives in plastic products ranging from intravenous fluid bags to children's toys, and antioxidant or stabilizer additive migration can often limit the useful service life of a product. The rate of diffusion or migration is usually a complex function of the size, shape, and flexibility of the small molecule,^{5–7} the free volume or mobility of the polymer matrix,^{8,9} temperature, and any specific interaction between the diffusing molecule and polymer.^{10–12}

There have been many studies^{13–18} of the effects of specific interactions on the rotational reorientation dynamics and translational diffusion of small molecule solute–small molecule solvent systems. Such effects yield deviations in observed dynamics from Stokes–Einstein (SE) or Debye–Stokes–Einstein (DSE) theories^{19–21} that are relatively small, often ranging from several percent to 50%.^{13,14} These studies have considered the effects of polar, ionic, and hydrogen-bonding interactions. The observed deviations from SE or DSE expectations associated with solute–solvent polarity effects have often been explained with modifications such as dielectric friction, i.e., the torque on a reorienting polar solute resulting from the induced polarization of the nearby solvent;¹³ among the most common dielectric friction models employed to account

for dielectric friction effects are those by Nee and Zwanzig²² and van der Zwan and Hynes²³ and modifications thereof. In contrast to polarity effects, hydrogen-bonding effects have sometimes been treated separately and have been explained as resulting from an increase in the volume of the reorienting molecule; usually, this explanation is qualitative rather than quantitative due to the difficulty in determining the volume of a solute–solvent complex.

There have also been studies of specific interaction effects in the case of polymer solutions. For example, hydrogen bonding has been found to slow probe translational diffusion^{24–29} and probe rotational motion²⁸ significantly in polymer/solvent systems. Related phenomena have been seen in a few limited studies of probe rotational motion in bulk polymer films,^{10–12} but a detailed understanding of these hydrogen-bonding effects is lacking in polymeric systems.

To predict and model diffusion effectively in these complex polymeric systems, a quantitative understanding of the role of hydrogen bonding is needed. In this study, we compare the translational and rotational diffusion of two small molecule probes, lophine and *S*-lophine, in bulk, amorphous polystyrene (PS) and poly(isobutyl methacrylate) (PiBMA) films (see Figure 1) near the glass transition temperature (T_g). The probes are essentially identical in size and shape with the only difference being that lophine is susceptible to secondary interactions with the polymer through an amine functional group. (As the most logical form of secondary interaction involving a probe containing an amine unit and a polymer such as PiBMA containing ester side groups is hydrogen bonding, we shall refer to the secondary interaction throughout the remainder of this paper as hydrogen bonding. This approach is consistent with that used in previous literature.^{24–28} For further

[†] Department of Chemical Engineering, Northwestern University.

[‡] IBM Almaden Research Center.

[§] Department of Materials Science and Engineering, Northwestern University.

* To whom correspondence should be addressed.

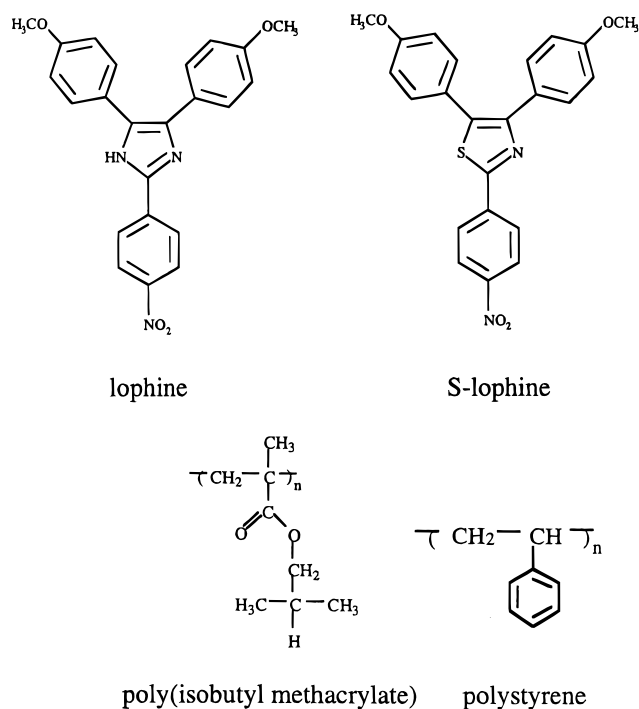


Figure 1. Probes and polymers used in this work.

comments, see ref 30.) This study will demonstrate the very substantial effects of hydrogen bonding in modifying small molecule probe dynamics in bulk polymers near T_g , and the results will be analyzed in terms of current theories of translational and rotational diffusion in polymeric systems with an emphasis placed on gaining physical insight into the nature of motion in these complex materials.

Experimental Section

Rotational Diffusion. Probe rotational diffusion was measured using second harmonic generation (SHG). Thin films (2–4 μm thick) of PS or PiBMA doped with either 1.2 mol % (4.8 wt %) probe (PS) or 1.7 mol % (4.8 wt %) probe (PiBMA) (moles of probe/moles of polymer repeat units) were spin-coated onto quartz slides upon which planar chrome electrodes had been patterned (800 μm gap). The films were then annealed under vacuum for 12 h at room temperature and at temperatures above the T_g of the polymer. After heating to the measurement temperature, the sample was poled by applying a 15 kV/cm dc field for approximately 60 s. This poling process aligns the dipoles of the probes and creates a noncentrosymmetric medium, which is required for second harmonic generation (frequency doubling) to occur. Upon removal of the field the dipoles are free to reorient back to a random distribution causing a decrease in SHG intensity. The second-order macroscopic susceptibility, $\chi^{(2)}$, is proportional to the orientation of the dipoles:

$$\chi^{(2)} \propto \sqrt{I(2\omega)} \propto \langle \cos \theta \rangle \quad (1)$$

where $I(2\omega)$ is SHG intensity and θ is the angle between the dc field and the probe dipole. SHG intensity was measured using a Q-switched Nd:YAG laser (10 Hz frequency) with a 1.064 mm fundamental beam. Probe reorientational dynamics from 5 μs to 2 s were measured using a variable time delay for switching off the dc field with respect to the laser pulse. Dynamics from 20 s onward were measured by monitoring SHG intensity after switching off the dc field permanently. More information on this technique can be found in ref 31.

The polymers used in the SHG studies were obtained from Scientific Polymer Products. PS ($M_n = 120\,000$; $M_w/M_n = 3.6$) had a $T_g = 100\text{ }^\circ\text{C}$ ($\pm 0.5\text{ }^\circ\text{C}$, DSC onset at $10\text{ }^\circ\text{C}/\text{min}$), and

PiBMA films ($M_n = 140\,000$; $M_w/M_n = 2.0$) had a $T_g = 54\text{ }^\circ\text{C}$. The addition of $>1\text{ mol } \%$ of probes for these measurements modified the T_g of the films only slightly:^{32,33} PS + 1.2 mol % lophine, $T_g = 98.5\text{ }^\circ\text{C}$; PS + 1.2 mol % S-lophine, $T_g = 98\text{ }^\circ\text{C}$; PiBMA + 1.7 mol % lophine, $T_g = 55\text{ }^\circ\text{C}$; PiBMA + 1.7 mol % S-lophine, $T_g = 53\text{ }^\circ\text{C}$.

Translational Diffusion. The translational diffusion of both probes was measured using fluorescence nonradiative energy transfer (NRET). Nonradiative energy transfer occurs when a "donor" transfers its excited-state energy to an "acceptor" through a dipole–dipole interaction over distances of a few nanometers. This results in a decrease in the fluorescence intensity of the donor which can be measured. In our experiments, lophine and S-lophine served as energy transfer acceptors, and pyrene, which had been covalently attached as a side group to a small fraction of the repeat units of the polymer, served as the energy transfer donor. Thin films (0.5–1 mm thick) of PS or PiBMA doped with between 0.1 and 0.4 mol % (0.3–1.6 wt %) of either lophine or S-lophine were spin-coated from dilute toluene solutions onto acid-cleaned fused quartz slides. Complementary films in which between 0.075 and 0.14 mol % of the polymer repeat units contained a covalently attached pyrene group were spin-coated from dilute toluene solutions onto glass slides. Films were then annealed for 24 h under vacuum at room temperature. Bilayer films were created by layering the pyrene containing donor films on top of the probe containing acceptor films via a water transfer method. The bilayer films were annealed for 24 h under vacuum at room temperature to remove any residual water. To prevent bleaching of the donor in PS films at elevated temperature, an additional PS film was layered on top of the donor layer. PS films ($M_n = 75\,000$; $M_w/M_n = 1.5$) had a $T_g = 100\text{ }^\circ\text{C}$ ($\pm 0.5\text{ }^\circ\text{C}$, DSC onset at $10\text{ }^\circ\text{C}/\text{min}$), and PiBMA films ($M_n = 200\,000$; $M_w/M_n = 2.0$, molecular weights relative to PMMA standards using THF as solvent and measurement via gel permeation chromatography) had a $T_g = 64\text{ }^\circ\text{C}$. For both polymers, T_g is essentially unchanged by the addition of amounts of probe molecules as used here. (The very low probe content³³ and the constancy of T_g of the polymer with probe addition ensure that these experiments characterize probe diffusion in the limit where diffusion as measurable by NRET due to the very small gradient in concentration is essentially equivalent to self-diffusion.) The $10\text{ }^\circ\text{C}$ difference in T_g between the PiBMA used in the NRET measurements and that used in the SHG measurements is consistent with the effect of polymerization temperature on polymer tacticity; such effects are known to have substantial impact on T_g in methacrylate-based polymers. These differences were found not to affect probe dynamics when normalized to T_g .^{34,35}

The bilayer films were then placed in a temperature-controlled sample cell in a Spex Fluorolog II spectrofluorimeter and heated to the measurement temperature. Upon reaching thermal equilibrium, the fluorescence emission intensity of the donor (pyrene) was measured as a function of time. The excitation wavelength used was 328 nm for PiBMA films and 331 nm for PS films. Emission wavelength was either 374 or 397 nm. Translational diffusion of the acceptor molecules (lophine or S-lophine) into the donor layer causes a net decrease in the fluorescence intensity of the donor layer due to nonradiative energy transfer. Assuming that the donor is immobile since it is covalently attached to the polymer matrix and that there is Fickian diffusion of the acceptor molecules, the acceptor translational diffusion coefficient, D , may be determined by measuring the decrease in donor fluorescence intensity due to nonradiative energy transfer as a function of time:⁵

$$E(t) = \frac{I(0) - I(t)}{I(0)} = K \left(\frac{\sqrt{Dt}}{w} \right) \quad \text{for } t \leq \frac{w^2}{16D} \quad (2)$$

where $E(t)$ is energy transfer efficiency, $I(0)$ and $I(t)$ are the initial donor fluorescence intensity and the donor intensity at time t , respectively, K is a constant that depends on the particular donor–acceptor pair employed and on the initial

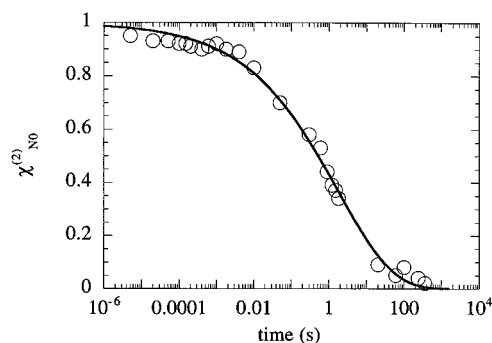


Figure 2. SHG decay for lophine in PS at $T = T_g + 4$ °C. Curve is fit to eq 3 with $\tau = 2.2$ s and $\beta = 0.30$.

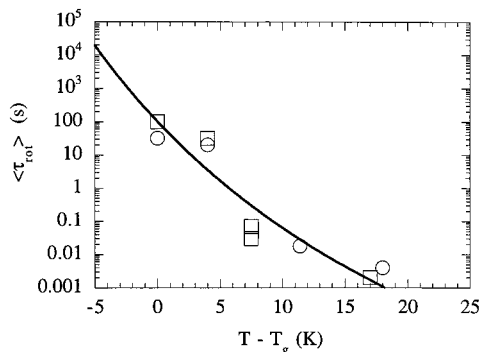


Figure 3. Temperature dependence of the rotational time constants of (○) lophine and (□) *S*-lophine in PS. Curve is fit to eq 5 with $C_1 = 16$, $C_2 = 40$ K, and $\tau_0 = 10^{-14}$ s.

acceptor concentration, and w is the donor layer thickness. We have also assumed that there is negligible diffusion before our initial intensity measurement at $t = 0$. More information on fluorescence NRET and its use in measuring diffusion in polymer films can be found in refs 5, 6, and 36.

Results and Discussion

The rotational motion of lophine and *S*-lophine was measured in PS and PiBMA using SHG. Figure 2 shows the decay in $\chi_{N0}^{(2)}$ ($\chi^{(2)}$ normalized to the value at $t = 0$) as a function of time for lophine in PS at $T = T_g + 4$ °C. The data may be fit to a Kohlrausch–Williams–Watts stretched exponential.^{37,38}

$$\chi_{N0}^{(2)} = \exp(-(t/\tau)^\beta) \quad (3)$$

where τ is the characteristic relaxation time and β is the stretching exponent. An average rotational reorientation relaxation time constant, $\langle\tau_{\text{rot}}\rangle$, may then be calculated:

$$\langle\tau_{\text{rot}}\rangle = \frac{\tau\Gamma(1/\beta)}{\beta} \quad (4)$$

where Γ is the gamma function.

$\langle\tau_{\text{rot}}\rangle$ as a function of temperature for lophine and *S*-lophine in PS is shown in Figure 3. Both probes exhibit very similar rotational dynamics in PS. This similarity is expected given the nearly identical size and shape of the molecule and the nonpolar nature of polystyrene, preventing any significant polymer–small molecule specific interactions. The rotational motion of large probes such as lophine and *S*-lophine has been shown previously to be coupled to the cooperative segmental mobility associated with the α -relaxation of the polymer matrix,^{7,31,39–41} which is known to have a

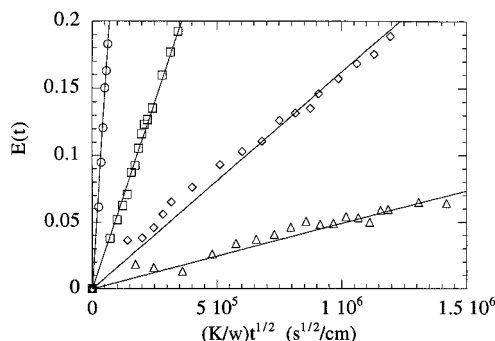


Figure 4. Energy transfer efficiency plot from eq 2 for lophine diffusion in PS at several different temperatures: (△) $T_g + 2$ °C, (◇) $T_g + 6.5$ °C, (□) $T_g + 12$ °C, (○) $T_g + 29$ °C. Slope = $D^{1/2}$.

very strong temperature dependence in the rubbery state near T_g . The $\langle\tau_{\text{rot}}\rangle$ results in Figure 3 are consistent with those showing the coupling of probe rotational motion to polymer α -relaxation dynamics. Therefore, the temperature dependence of $\langle\tau_{\text{rot}}\rangle$ follows a Vogel–Fulcher–Tamann (VFT)⁴² or equivalently a Williams–Landel–Ferry (WLF)⁴³ form:

$$\langle\tau_{\text{rot}}\rangle = \tau_0 \exp\left(\frac{2.303C_1C_2}{C_2 + T - T_g}\right) \quad (5)$$

where τ_0 is a microscopic parameter associated with the frequency of barrier hopping⁴⁴ and is expected to have “phonon-like” time scales, $\sim 10^{-14}$ s, and C_1 and C_2 are the WLF parameters of the polymer matrix. Values for C_1 and C_2 are typically found from measurements of the temperature dependence of polymer viscosity or dielectric relaxation. For commonly studied polymers, there are often a number of published values from which to choose. The question then becomes, which are the most appropriate? Recently, Angell⁴⁵ has proposed that there is a physical basis for assuming $C_1 = 16$ when the reference temperature in the WLF equation is taken as T_g . Angell has shown that

$$C_1 = \log(\tau_g/\tau_0) \quad (6)$$

where τ_g is the relaxation time at T_g . At the 10 °C/min DSC determined T_g , it has been shown that $\tau_g \sim 100$ s, and thus $C_1 \sim 16$ if one assumes $\tau_0 = 10^{-14}$ s. C_2 then reflects the “fragility” of the polymer, with lower C_2 values indicating a more fragile, i.e., more temperature dependent, system. For the probe rotation data in Figure 3, we will thus assume $C_1 = 16$ and $\tau_0 = 10^{-14}$ s and use C_2 as our fitting parameter. This procedure yields $C_2 = 40$ K and gives an adequate fit to the experimental data.

The translational diffusion coefficients of lophine and *S*-lophine were measured in PS using fluorescence NRET. $E(t)$ as a function of $(K/w)t^{1/2}$ for lophine diffusion in PS at several different temperatures is shown in Figure 4. The linearity of each plot is consistent with eq 2 with the slope and thus D increasing with temperature. The temperature dependence of D for both lophine and *S*-lophine is given in Figure 5. Each data point in Figure 5 is the average of at least three different film samples with error being reflected in the size of the symbols. The measured D values for both probes are essentially identical over the temperature range studied with D increasing by about 4 orders of magni-

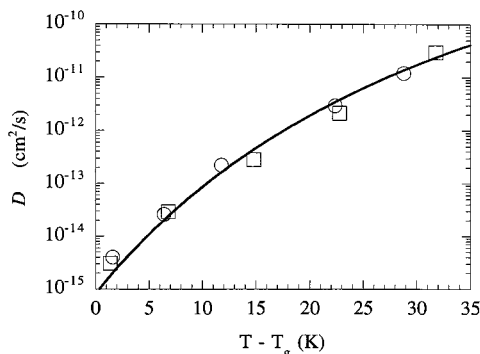


Figure 5. Temperature dependence of the translational diffusion coefficients of (○) lophine and (□) *S*-lophine in PS. Curve is fit to eq 7 with $C_1 = 16$, $C_2 = 40\text{K}$, $D_0 = 10^{-5}\text{ cm}^2/\text{s}$, $E_a = 0$, and $\xi = 0.63$.

tude as temperature is increased 30 °C. Although smaller than the temperature dependence of $\langle\tau_{\text{rot}}\rangle$, the nevertheless dramatic change in D with temperature is typical of free-volume-limited diffusion near T_g .

Many theoretical descriptions of translational diffusion in polymer systems revolve around the concept of free volume. The most well accepted of these is the Vrentas–Duda free volume theory.^{46–49} For tracer diffusion in bulk polymer systems, the theory predicts the following for the temperature dependence of D :

$$D = D_0 \exp\left(\frac{-E_a}{RT}\right) \exp\left(\frac{-2.303\xi C_1 C_2}{C_2 + T - T_g}\right) \quad (7)$$

where D_0 is a temperature-independent constant, E_a is the activation energy required for the probe to escape from its neighbors and make a diffusive jump, and R is the gas constant. The parameter ξ has been interpreted by Vrentas and Duda as being the ratio of the “jumping unit size” of the probe to that of the polymer involved in diffusive steps. (It must be noted that this interpretation does not necessitate that a probe “jump” requires a movement of the whole probe into a new volume; instead, only a fraction of the probe may need to move into space not occupied by probe prior to the diffusive step.^{50–53}) Specific interactions between the probe and polymer, such as hydrogen bonding, would be accounted for in the magnitude of E_a . In the absence of specific interactions, the energy term is often neglected since it is much smaller than the free volume term for temperatures near T_g .^{46–49}

For the translational diffusion of lophine and *S*-lophine in PS, no specific interaction between the probes and polymer is expected since PS has no hydrogen bond acceptor groups. We may then assume that $E_a = 0$. The parameters D_0 and ξ are more ambiguous. From eq 7, we see that as $T \rightarrow \infty$, $D \rightarrow D_0$. D_0 may be viewed as the diffusion coefficient in the absence of free volume limitations and thus only dependent on the properties of the probe molecule.^{46–49} For solvent diffusion, it may be estimated from pure solvent viscosity and density data.^{46–49} Values on the order of 10^{-3} – $10^{-4}\text{ cm}^2/\text{s}$ are typically reported with no obvious dependence on solvent size.^{46–49} Dye diffusion in bulk polymer films near T_g has been studied by Ehlich and Sillescu,⁸ who have taken an alternative view of this parameter. They treat it as a parameter that is dependent on both the fractional free volume of the polymer at T_g and also the “coupling” of probe diffusion to the α -relaxation of the polymer matrix; however, its value must be calculated

from measured diffusion data and has little physical meaning. Their values for D_0 ranged from 10^7 to $10^{-5}\text{ cm}^2/\text{s}$. It is desirable to provide a physical basis for this parameter for probe diffusion in bulk polymer systems. One might expect that at high temperatures D should approach values typical for probe diffusion in low molecular weight liquids; thus, $D_0 \sim 10^{-5}\text{ cm}^2/\text{s}$.^{24–26,54} The exact value depends on probe size and fluid viscosity but is generally between 1×10^{-5} and $3 \times 10^{-5}\text{ cm}^2/\text{s}$ for most systems. Values can also be estimated from the Stokes–Einstein equation and the Wilke–Chang correlation.⁵⁴ In the interest of reducing the number of parameters used to “fit” the data and also to provide some physical basis to D_0 , we shall assume $D_0 = 10^{-5}\text{ cm}^2/\text{s}$ for the probes studied here.

A comparison of eqs 5 and 7 indicates that, in the absence of specific interactions, the difference in temperature dependencies of $\langle\tau_{\text{rot}}\rangle$ and D can be attributed to the parameter ξ . The value of ξ is dependent on not only the size of the probe but also its shape and flexibility; as well, the dynamics of the polymer matrix related to the length scale of the cooperatively rearranging regions of the α -relaxation, generally believed to be on the order of several nanometers,^{55,56} should also affect the value of ξ . Therefore, it depends on both the characteristics of the probe and the polymer matrix. Ehlich and Sillescu⁸ have also interpreted the value of ξ as reflecting the degree of coupling of probe translational motion to the α -relaxation of the polymer, with larger ξ values, approaching 1, implying a greater coupling between probe motion and polymer relaxation.

On this basis, one might expect that since the rotational motions of lophine and *S*-lophine are fully coupled to the α -relaxation of the polymer matrix, as exhibited in Figure 3, then translational diffusion should likewise be fully coupled, i.e., $\xi = 1$ in eq 7. Previous studies by several groups^{5–8,57–61} have shown, in agreement with the results presented here, that this is apparently not true; D is less temperature dependent than $\langle\tau_{\text{rot}}\rangle$ in the rubbery state near T_g , i.e., $\xi < 1$ in eq 7. As T is cooled toward T_g , the average distance a probe translates in one average rotational relaxation time becomes larger and larger, and it appears that translational motion becomes enhanced compared to rotation as T_g is approached. The reason for this apparent paradox can be linked to the presence of spatially heterogeneous dynamics near T_g .^{57–63} Dynamic heterogeneities are regions that relax at different time scales from one another and are manifested in the extremely broad distribution of relaxation times present in these materials near T_g .⁶¹ Translation and rotation measurements average over this broad distribution of relaxation times differently. The rotation experiments give a “snapshot” of the distribution, and calculation of $\langle\tau_{\text{rot}}\rangle$ is dominated by the slowest relaxing regions which make up the portion of the distribution most often associated with α -relaxation processes. In the translation experiments, each probe may experience many different environments during the course of the measurement, and the calculated D value will be dominated by the fast relaxing regions where the probe translates most rapidly. As the material is cooled toward T_g , the relaxation time distribution broadens (β in eq 3 decreases). This broadening occurs primarily on the fast-time portion of the distribution, thus causing the fast-time portion to be less temperature dependent than the slow-time portion.⁶¹ The apparent enhancement in

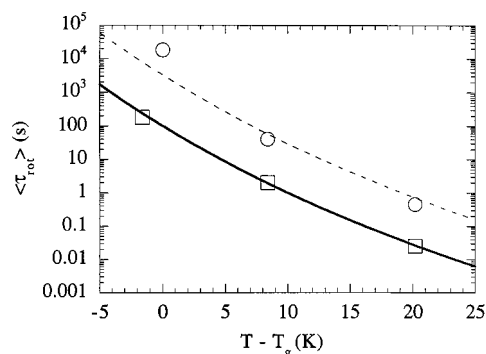


Figure 6. Temperature dependence of the rotational time constants of (○) lophine and (□) *S*-lophine in PiBMA. Solid curve is fit to eq 5 with $C_1 = 16$, $C_2 = 70\text{K}$, and $\tau_0 = 10^{-14}$ s. Dashed curve is fit to eq 8 with $C_1 = 16$, $C_2 = 70\text{K}$, $\tau_0 = 10^{-14}$ s, and $E_a = 9.5$ kJ/mol.

translational diffusion is therefore a direct result of the broadening of the relaxation time distribution and how the measurement averages over the heterogeneous dynamics, not any decoupling of translational motion from polymer relaxation.⁶¹ This interpretation is further supported by the observation that D and $\langle \tau_{\text{rot}} \rangle$ recover similar temperature dependencies in the quenched glassy state near T_g where the distribution of α -relaxation processes is observed to have essentially a temperature-independent breadth and merely shifts to longer times at lower temperature.⁶¹

The complexity of the ξ parameter for diffusion in bulk polymer systems near T_g makes its a priori prediction tenuous at best; therefore, we will use it as a fitting parameter for our data. The solid curve in Figure 5 is a fit to eq 7 with $\xi = 0.63$ and assuming $C_1 = 16$, $C_2 = 40\text{K}$, and $D_0 = 10^{-5}$ cm²/s. It gives an excellent fit to both the lophine and *S*-lophine data in the temperature range examined.

The rotational relaxation behaviors of lophine and *S*-lophine were also measured in PiBMA near T_g , and the temperature dependence of $\langle \tau_{\text{rot}} \rangle$ is shown in Figure 6. In contrast to the results for PS in Figure 3, there is a large difference in $\langle \tau_{\text{rot}} \rangle$ values between lophine and *S*-lophine in PiBMA, with the values for lophine being at least an order of magnitude slower than for *S*-lophine at equivalent temperatures. (These effects are much larger than those attributable to specific interactions in solute-solvent systems or in polymer solutions.) Due to the presence of the carbonyl moiety in the methacrylate side group, PiBMA can serve as a hydrogen bond acceptor for the amine functionality on lophine. Such hydrogen bonding between the lophine probe and the PiBMA matrix would be expected to hinder significantly the rotational motion of the probe. The *S*-lophine data in Figure 6 may be adequately fit using eq 5 with $C_2 = 70\text{K}$ while assuming $C_1 = 16$ and $\tau_0 = 10^{-14}$ s. This value for C_2 makes sense because PiBMA is known to be less "fragile" than PS.³⁹ The lophine data cannot be fit with eq 5 using our current assumptions, and we must add an activation energy term such as is found in eq 7 to account for the interaction between the lophine and PiBMA:

$$\langle \tau_{\text{rot}} \rangle = \tau_0 \exp\left(\frac{E_a}{RT}\right) \exp\left(\frac{2.303C_1C_2}{C_2 + T - T_g}\right) \quad (8)$$

where E_a is the interaction energy barrier that the probe must overcome before undergoing rotational motion.

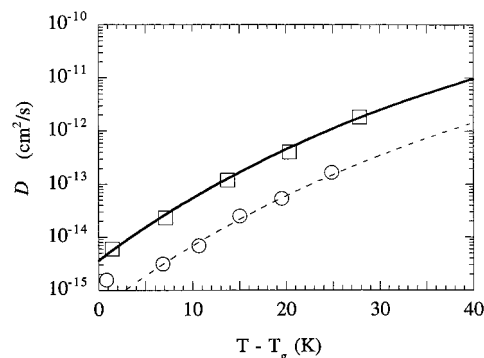


Figure 7. Temperature dependence of the translational diffusion coefficients of (○) lophine and (□) *S*-lophine in PiBMA. Solid curve is fit to eq 7 with $C_1 = 16$, $C_2 = 70\text{K}$, $D_0 = 10^{-5}$ cm²/s, $E_a = 0$, and $\xi = 0.59$. Dashed curve is fit to eq 7 with the same parameters except $E_a = 6$ kJ/mol.

The lophine data in Figure 6 are fit to eq 8 with $E_a = 9.5$ kJ/mol while assuming $C_1 = 16$, $C_2 = 70\text{K}$, and $\tau_0 = 10^{-14}$ s. This value for E_a compares favorably to values typically associated with hydrogen bonding of between 8 and 40 kJ/mol.⁶⁴

Figure 7 plots D as a function of temperature for lophine and *S*-lophine translational diffusion in PiBMA. Consistent with the rotational diffusion data in Figure 6, we find that lophine translational diffusion is approximately an order of magnitude slower than *S*-lophine in PiBMA. *S*-Lophine diffusion in Figure 7 may be fit using eq 7 with $\xi = 0.59$ ⁶⁵ and assuming $E_a = 0$, $C_1 = 16$, $C_2 = 70\text{K}$, and $D_0 = 10^{-5}$ cm²/s. We can no longer assume that $E_a = 0$ for lophine diffusion in PiBMA due to the presence of hydrogen bonding. If we assume that both ξ and D_0 are independent of specific interactions between the probe and polymer, then $\xi = 0.59$ and $D_0 = 10^{-5}$ cm²/s for lophine diffusion in PiBMA, and E_a may be used as our fitting parameter. The lophine data in Figure 7 are adequately fit with $E_a = 6$ kJ/mol.

The reason for E_a for rotation being more than 50% larger than that for translation may be traced again to how the two measurements of probe motion average over the distribution of environments in the polymer matrix. Values of $\langle \tau_{\text{rot}} \rangle$ are influenced primarily by the probes with the slowest rotation times which are presumably those that are strongly hydrogen bonded with the matrix. In contrast, D values are influenced most by the fastest relaxing environments with the fastest moving probes, which are presumably those probes that have experienced less hindrance due to hydrogen bonding in the course of their translation. In other words, while D characterizes the diffusion of all probes averaged over time scales long with respect to $\langle \tau_{\text{rot}} \rangle$ (so that all probes participate in translational diffusion and experience over time both fast and slow local relaxation environments, associated in part with low and significant hydrogen bonding, respectively), the translational diffusion coefficient primarily reflects the fast relaxing, low hydrogen-bonding local environments.

A final comment must be made regarding the role of hydrogen-bonding effects in extending the useful life of polymers with additives. As discussed earlier, the seemingly paradoxical behavior of probe translational diffusion being less temperature dependent than rotational dynamics (coupled to the polymer α -relaxation dynamics) in the rubbery state near T_g may lead to migration of additives in the polymer enhanced much beyond

expectations based on a temperature dependence from SE^{20,21} theory. For example, actual diffusion coefficients at T_g can be as much as 5–6 orders of magnitude larger than those expected on the basis of SE scaling.^{8,66} (Such paradoxical effects have only very recently become known with the first report made in 1992⁶⁷ for low-molecular-weight glass formers.) As a result, the useful service life of a polymer may be far shorter than anticipated if additive migration has a negative impact on polymer properties. While specific interactions, such as hydrogen bonding, between the small molecule additives and polar polymers in no way eliminate this translation–rotation paradox, as evidenced by $\xi = 0.59$ for both lophine and *S*-lophine in PiBMA, the fact that D is decreased by approximately an order of magnitude in the case of lophine in PiBMA as compared to *S*-lophine in PiBMA indicates that service life of bulk polymer products may be greatly enhanced by taking advantage of specific interaction effects. In particular, if service life is limited by additive migration, migration distance will be reduced by more than a factor of 3 for every order of magnitude reduction in D ; in the case considered here, the service life of a hydrogen-bonded lophine–PiBMA system could be an order of magnitude larger than that of an *S*-lophine–PiBMA system.

Conclusions

In this work, we have studied the translational and rotational diffusion of two small molecule probes in bulk polymer films near T_g . The probes are of essentially identical size and shape with the only difference being their ability to hydrogen bond to the polymer matrix. Hydrogen bonding was found to slow significantly both probe translational and rotational diffusion. The magnitude of the effect is much greater than those typically reported for diffusion in polymer–solvent solutions and could be used as a strategy to prolong the life of polymer systems affected deleteriously by additive migration. Translational diffusion results could be adequately represented by Vrentas–Duda free volume theory with hydrogen bonding being taken into account through the interaction energy term with $E_a = 6$ kJ/mol. The rotational motion of both probes was found to follow the α -relaxation temperature dependence of the polymer host. For rotation, hydrogen bonding could also be accounted for using an interaction energy term with $E_a = 9.5$ kJ/mol. The differences in interaction energy values for the two modes of motion can be explained in terms of how average measures of translation and rotation weight different portions of the broad relaxation time distributions present in these systems.

Acknowledgment. We gratefully acknowledge Denise D. Deppe for synthesis of the pyrene-labeled PS and PiBMA. D.B.H. also acknowledges the receipt of a Northwestern University Dissertation Year Cabell Fellowship. This work was supported by the MRSEC program of the National Science Foundation (DMR-9632472) at the Northwestern University Materials Research Center.

References and Notes

- (1) Foldes, E. *Angew. Makromol. Chem.* **1998**, 262, 65.
- (2) Saltzman, W. M.; Radomsky, M. L. *Chem. Eng. Sci.* **1991**, 46, 2429.
- (3) Burland, D. M.; Miller, R. D.; Walsh, C. A. *Chem. Rev.* **1994**, 94, 31.
- (4) Prasad, P. N.; Williams, D. J. *Introduction to Nonlinear Optical Effects in Molecules and Polymers*; Wiley: New York, 1991.
- (5) Deppe, D. D.; Dhinojwala, A.; Torkelson, J. M. *Macromolecules* **1996**, 29, 3898.
- (6) Deppe, D. D.; Miller, R. D.; Torkelson, J. M. *J. Polym. Sci., Polym. Phys.* **1996**, 34, 2987.
- (7) Hall, D. B.; Deppe, D. D.; Hamilton, K. E.; Dhinojwala, A.; Torkelson, J. M. *J. Non-Cryst. Solids* **1998**, 235–237, 48.
- (8) Ehlich, D.; Sillescu, H. *Macromolecules* **1990**, 23, 1600.
- (9) Von Meerwall, E.; Skowronski, D.; Hariharan, A. *Macromolecules* **1991**, 24, 2441.
- (10) Hampsch, H. L.; Yang, J.; Wong, G. K.; Torkelson, J. M. *Polym. Commun.* **1989**, 30, 40.
- (11) Wright, M. E.; Mullick, S.; Lackritz, H. S.; Liu, L. Y. *Macromolecules* **1994**, 27, 3009.
- (12) Pace, M. D.; Snow, A. W. *Macromolecules* **1995**, 28, 5300.
- (13) Dutt, G. B.; Singh, M. K.; Sapre, A. V. *J. Chem. Phys.* **1998**, 109, 5994.
- (14) Dutt, G. B.; Doraiswamy, S.; Periasamy, N.; Venkatavaman, G. *J. Chem. Phys.* **1990**, 93, 8498.
- (15) Alavi, D. S.; Hartman, R. S.; Waldeck, D. H. *J. Chem. Phys.* **1991**, 94, 4509.
- (16) Hartman, R. S.; Konitsky, W. M.; Waldeck, D. H.; Chang, Y. J.; Castner, E. W. *J. Chem. Phys.* **1997**, 106, 7920.
- (17) Horng, M. L.; Gardecki, J. A.; Maroncelli, M. *J. Phys. Chem. A* **1997**, 101, 1030.
- (18) Mikosch, W.; Dorfmueller, T.; Elmer, W. *J. Chem. Phys.* **1994**, 101, 11044.
- (19) Debye, P. *Polar Molecules*; Dover: New York, 1928.
- (20) Einstein, A. *Ann. Phys. (Leipzig)* **1906**, 19, 289.
- (21) Stokes, G. *Trans. Cambridge Philos. Soc.* **1856**, 9, 5.
- (22) Nee, T. W.; Zwanzig, R. *J. Chem. Phys.* **1970**, 52, 6353.
- (23) van der Zwan, G.; Hynes, J. T. *J. Phys. Chem.* **1985**, 89, 4181.
- (24) Lee, J. A.; Lodge, T. P. *J. Phys. Chem.* **1987**, 91, 5546.
- (25) Lee, J.; Park, K.; Chang, T.; Jung, J. C. *Macromolecules* **1992**, 25, 6977.
- (26) Park, H. S.; Sung, J.; Chang, T. *Macromolecules* **1996**, 29, 3216.
- (27) Sung, J.; Chang, T. *Polymer* **1993**, 34, 3741.
- (28) Ilyina, E.; Daragan, V. A.; Prisman, A. E. *Macromolecules* **1993**, 26, 3319.
- (29) Hall, D. B.; Torkelson, J. M. *Macromolecules* **1998**, 31, 8817.
- (30) Confirmation of the presence of hydrogen bonding through infrared spectroscopy was attempted; however, for the low probe levels used here, assignment of functional group peaks involved in hydrogen bonding could not be done with the required accuracy.
- (31) Dhinojwala, A.; Wong, G. K.; Torkelson, J. M. *Macromolecules* **1993**, 26, 5943.
- (32) PiBMA has not shown substantial plasticization effects on T_g for the probes studied in our group (see ref 41) even up to loadings of 10 wt % probe, so it is not surprising that T_g is basically unaffected by the addition of 4.8 wt % of lophine or *S*-lophine. We have found the T_g of PS to be more susceptible to plasticization effects than PiBMA, and the results given here are consistent with that observation.
- (33) UV/vis spectroscopy showed no significant probe aggregation (no broadening of the spectrum with increasing concentration) for the concentrations used here. Assuming a uniform distribution of probes in the polymer matrix, the average separation distance between each probe is approximately 2 nm for the highest concentration employed (4.8 wt %).
- (34) Dhinojwala, A.; Hooker, J. C.; Torkelson, J. M. *J. Non-Cryst. Solids* **1994**, 172–174, 286.
- (35) Even in different methacrylate-based polymers such as PiBMA and poly(ethyl methacrylate), within error, SHG probe dynamics have been found to be identical when normalized to T_g . See ref 31.
- (36) Dhinojwala, A.; Torkelson, J. M. *Macromolecules* **1994**, 27, 4817.
- (37) Kohlrausch, R. *Ann. Phys. (Leipzig)* **1847**, 12, 393.
- (38) Williams, G.; Watts, D. C. *Trans. Faraday Soc.* **1970**, 66, 80.
- (39) Dhinojwala, A.; Wong, G. K.; Torkelson, J. M. *J. Chem. Phys.* **1994**, 100, 6046.
- (40) Hooker, J. C.; Torkelson, J. M. *Macromolecules* **1995**, 28, 7683.
- (41) Hamilton, K. E. Ph.D. Thesis, Northwestern University, 1996.
- (42) Vogel, H. J. *Phys. Z.* **1921**, 22, 645. Fulcher, G. S. *J. Am. Ceram. Soc.* **1925**, 8, 339. Tammann, G.; Hesse, W. *Z. Anorg. Allg. Chem.* **1926**, 156, 245.
- (43) Williams, M. L.; Landel, R. F.; Ferry, J. D. *J. Am. Chem. Soc.* **1955**, 77, 3701.

- (44) Adam, G.; Gibbs, J. H. *J. Chem. Phys.* **1965**, *43*, 139.
- (45) Angell, C. A. *Polymer* **1997**, *38*, 6261.
- (46) Vrentas, J. S.; Duda, J. L. *J. Polym. Sci., Polym. Phys. Ed.* **1977**, *15*, 403.
- (47) Duda, J. L.; Vrentas, J. S.; Ju, S. T.; Liu, H. T. *AIChE J.* **1982**, *28*, 279.
- (48) Zielinski, J. M.; Duda, J. L. *AIChE J.* **1992**, *38*, 405.
- (49) Vrentas, J. S.; Vrentas, C. M. *Eur. Polym. J.* **1998**, *34*, 797.
- (50) Arnould, D.; Lawrence, R. L. *Ind. Eng. Chem. Res.* **1992**, *31*, 218.
- (51) Vrentas, J. S.; Vrentas, C. M.; Faridi, N. *Macromolecules* **1996**, *29*, 3272.
- (52) Wisnudel, M. B.; Torkelson, J. M. *Macromolecules* **1996**, *29*, 6193.
- (53) Such diffusive movement of a probe molecule in which a diffusive step involves a step of only a fraction of the probe molecular volume can be easily accommodated by cooperative segmental mobility of the polymer matrix.
- (54) Wisnudel, M. B.; Torkelson, J. M. *AIChE J.* **1996**, *42*, 1157.
- (55) Fischer, E. W.; Donth, E.; Steffan, W. *Phys. Rev. Lett.* **1992**, *68*, 2344.
- (56) Arndt, M.; Stannarius, R.; Groothues, H.; Hempel, E.; Kremer, F. *Phys. Rev. Lett.* **1997**, *79*, 2077.
- (57) Blackburn, F. R.; Cicerone, M. T.; Hietpas, G.; Wagner, P. A.; Ediger, M. D. *J. Non-Cryst. Solids* **1994**, *172-174*, 256.
- (58) Cicerone, M. T.; Blackburn, F. R.; Ediger, M. D. *J. Chem. Phys.* **1995**, *102*, 471.
- (59) Cicerone, M. T.; Blackburn, F. R.; Ediger, M. D. *Macromolecules* **1995**, *28*, 8224.
- (60) Cicerone, M. T.; Ediger, M. D. *J. Chem. Phys.* **1996**, *104*, 7210.
- (61) Hall, D. B.; Dhinojwala, A.; Torkelson, J. M. *Phys. Rev. Lett.* **1997**, *79*, 103.
- (62) Sillescu, H. *J. Non-Cryst. Solids* **1999**, *243*, 81.
- (63) Ediger, M. D.; Angell, C. A.; Nagel, S. R. *J. Phys. Chem.* **1996**, *100*, 13200.
- (64) Levine, I. N. *Physical Chemistry*, 3rd ed.; McGraw-Hill: New York, 1988.
- (65) The differences in $\xi = 0.63$ for PS and $\xi = 0.59$ for PiBMA are significant when one assumes D_0 is not dependent on the properties of the polymer matrix. The differences in ξ for the two polymer types may be related to differences in their short-time relaxation. Here, ξ is assumed to be constant over the temperature range studied; however, it may also be taken as being dependent on temperature since the shape of the polymer relaxation distribution is temperature dependent near T_g . At high temperatures, $T > \sim 1.2T_g$, where the relaxation distribution is its narrowest and its breadth is no longer significantly temperature dependent, ξ should approach 1.
- (66) Bainbridge, D.; Ediger, M. D. *Rheol. Acta* **1997**, *36*, 209.
- (67) Fujara, F.; Geil, B.; Sillescu, H.; Fleischer, G. *Z. Phys. B: Condens. Matter* **1992**, *88*, 195.

MA9904159